NASA TN D-1246

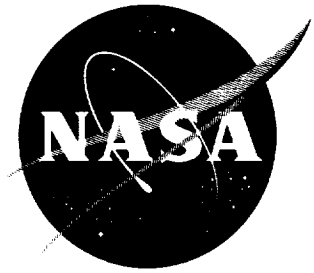

TECHNICAL NOTE

D-1246

PRESSURE MEASUREMENTS ON TWO 60° SWEPT DELTA WINGS WITH BLUNT LEADING EDGES AND DIHEDRAL ANGLES OF 0° AND 45° AT A MACH NUMBER OF 4.95

By P. Calvin Stainback

Langley Research Center
Langley Station, Hampton, Va.

NATIONAL AERONAUTICS AND SPACE ADMINISTRATION

WASHINGTON April 1962

NATIONAL AERONAUTICS AND SPACE ADMINISTRATION

TECHNICAL NOTE D-1246

PRESSURE MEASUREMENTS ON TWO 60° SWEPT DELTA WINGS WITH BLUNT LEADING EDGES AND DIHEDRAL ANGLES OF 0° AND 45° AT A MACH NUMBER OF 4.95

By P. Calvin Stainback

SUMMARY

An experimental investigation was conducted to measure the pressures on two 60° swept delta wings with cylindrical leading edges of 0.25-inch radii and dihedral angles of 0° and 45°. The tests were conducted at a Mach number of 4.95 and a stagnation temperature of 400° F. The test-section unit Reynolds number was 15.19×10^6 and the angle of attack was varied from 0° to 20°.

The results of the investigation indicated that, in general, Newtonian theory would not predict the pressure distribution on the model in a plane normal to the leading edge for angles of attack greater than zero. A method which utilizes a linear combination of viscous and inviscid pressure terms, developed by Creager for predicting pressures on blunt-leading-edge delta wing at angles of attack, was in good agreement with the measured pressure distributions. The stagnation-line pressure level could be predicted within ±9 percent by using the ideal-gas normal-shock relationship with the normal component of the free-stream Mach number.

INTRODUCTION

The use of large dihedral was proposed in reference 1 as a means of alleviating the leading-edge heating problem of delta wings at angle of attack. In order to evaluate this proposal, an experimental program has been conducted at the Langley Research Center to investigate the effects of dihedral on the aerodynamic characteristics of delta wings. Reference 2 presented heat-transfer data on two 60° swept delta wings with blunt leading edges and dihedral angles of 0° and 45° at a Mach number of 4.95. In order to analyze the heat-transfer data in reference 2, it was necessary to assume a pressure distribution. This distribution was obtained from Newtonian flow based on the Mach number

component normal to the leading edge. It is the purpose of the present paper to present measured pressure data for the wings tested in reference 2 to evaluate the validity of the assumed pressure distributions.

SYMBOLS

The symbols are defined with the aid of figure 1 which presents a schematic picture of a delta wing with dihedral and at an angle of attack. The complete wing with dihedral OABG is shown on the right in figure 1. The wing is symmetrical about line OB which is in the plane of the X- and Z-axis. The sweepback of the wing is defined as the complement of the semiapex angle. Also shown with the dihedral wing is a reference plane OA'BG' which passes through OB and is perpendicular to the plane of the X- and Z-axis. Dihedral is measured from the reference plane in a plane perpendicular to OB. On the left in figure 1, half of the wing with dihedral OAB and a portion of the reference plane OA'B are shown, together with some of the angles used in the discussion.

M	free-stream Mach number in direction of positive X-axis
p	pressure
r	wing leading-edge radius in plane normal to leading edge
s	distance along wing surface (at all angles of attack s is measured from the leading-edge stagnation line at $\alpha = 0^{\circ}$)
V	free-stream velocity in direction of positive X-axis
V_N	component of free-stream velocity normal to leading edge of wing and located in plane formed by the wing leading edge and the free-stream velocity
V_P	component of free-stream velocity along leading edge of wing
X,Y,Z	rectangular coordinate axes (fig. 1)
α	angle of attack of ridge line OB
α_{ϵ_e}	angle of attack at which effective sweeps of leading edge OA and ridge line OB are equal
α'	angle of attack of plane AOG of leading edges, angle XOH, planform angle of attack

Γ	dihedral angle
δ	angle between plane of velocity vectors EFODAC and plane of wing OAB, flow-deflection angle
δ_{max}	maximum flow turning angle for an attached shock in two-dimensional flow
ϵ_e	angle between leading edge OA and free-stream direction (X-axis), effective semiapex angle
ϵ_n	angle between ridge line OB and plane of leading edges AOG, angle BOH
ϵ_o	angle between leading edge OA and ridge line OB of wing, panel semiapex angle
ϵ_p	half of angle between leading edge OA and OG, angle AOH, planform semiapex angle
θ	angle between radius vector to surface and normal component of free-stream velocity
Λ_e	complement of ϵ_e, effective sweep
Λ_o	complement of ϵ_o, panel sweep

Subscripts:

N	normal to leading edge
s = 0	leading-edge stagnation line at $\alpha = 0^o$
sl	stagnation line
t	stagnation value
th	theoretical
P	parallel to plane of symmetry of model
∞	free-stream conditions
eff	effective
max	maximum

Superscript:

conditions behind normal shock

MODELS AND TEST PROCEDURE

Models

The models were 60° swept delta wings with blunt leading edges and dihedral angles of 0° and 45°. The leading-edge radii normal to the leading edges were 0.25 inch. The models were formed from identical wing panels and dihedral was introduced into the 45° dihedral model by rotating the wing panels about the line formed by the vertical plane of symmetry and the lower surfaces of the wing. This method of introducing dihedral was denoted as the constant panel case (ϵ_o = Constant) in reference 1. The ridge line of the 45° dihedral model was sharp and was not instrumented. L 1 3 2 4

The models were fabricated from 0.050-inch-thick stainless-steel sheet stock to the dimensions given in figure 2. The models were formed from two separate wing panels which were assembled by welding along the plane of symmetry. Pressure orifices, 0.040 inch in diameter, were located at two stations on the models. One station was parallel to the ridge line of the model; the other was located normal to the wing leading edge. Location of the individual orifices is shown in figure 2. Additional physical characteristics of the models are presented in table I.

Test Procedure and Recording and Reduction of Data

Testing of the models was conducted at the Langley Research Center in a 9-inch axially symmetric, continuous running, blowdown jet at a nominal Mach number of 4.95 and a stagnation temperature of 400° F. The test-section unit Reynolds number was 15.19×10^6 per foot and the angle of attack was varied from 0° to 20°.

The model orifice pressures were measured with a 120-inch mercury manometer or a butyl phthalate manometer, depending on the pressure level. The butyl phthalate manometer board sumps were evacuated to approximately the measured pressures to increase the response of the manometers. The sump pressure was indicated on a single-leg mercury manometer that was vented to the atmosphere.

The pressure distribution around the model, normal to the leading edge, was nondimensionalized by dividing the measured pressures by the

theoretical stagnation-line pressure calculated from the normal component of the free-stream Mach number normal to the leading edge. The origin of the coordinate system ($s = 0$) normal to the leading edge was taken as the stagnation line at zero angle of attack, and the pressure ratios were plotted as a function of the normal distance from $s = 0$ along the model surface. The pressure levels at $s = 0$ and at the stagnation line were nondimensionalized by dividing these pressures by the tunnel free-stream stagnation pressure; these results were plotted as a function of angle of attack.

DISCUSSION OF RESULTS

Pressure Distribution

The pressure distribution normal to the leading edge around the 0° and 45° dihedral models is presented in figures 3 and 4. The Newtonian pressure distributions calculated for the model by utilizing the Mach number component normal to the leading edge are shown in the figures. The Newtonian pressure distribution was assumed to be given by the following:

$$\frac{p}{p_t'} = \cos^2\theta + \frac{p_\infty}{p_t'} \sin^2\theta \tag{1}$$

The pressure ratio p_∞/p_t' was obtained from the normal-shock relationship for the Mach number component normal to the leading edge. The normal component of the Mach number is given by

$$M_N = M_\infty \cos \Lambda_e \tag{2}$$

where Λ_e is (from ref. 1):

$$\Lambda_e = \sin^{-1}\left(\cos \epsilon_o \cos \alpha + \sin \epsilon_o \sin \alpha \sin \Gamma\right) \tag{3}$$

The pressure-distribution data were presented as a function of the distance from $s = 0$; and since the stagnation line shifts from $s = 0$ at angle of attack, the theoretical distribution curve must be displaced along the s-axis to account for this shift. For an isolated swept cylinder, the shift in the stagnation line with angle of attack would be

equal to the flow-deflection angle δ given in reference 1 as:

$$\cos \delta = \frac{\cos \alpha - \cos \epsilon_o \cos \epsilon_e}{\sin \epsilon_o \sin \epsilon_e} \tag{4}$$

By using the assumption that the stagnation-line shift on the leading edge of a swept delta wing will, for low angles of attack, be equal to that of a swept cylinder, the theoretical distribution curves must be translated in the $(s/r)_n$ direction an amount δ (in radians) to account for the shift in the stagnation line with angle of attack.

The agreement between the experimental data and the Newtonian curves shown in figures 3 and 4 was very good at zero angle of attack for both the 0° and 45° dihedral models. At angles of attack greater than zero, the pressure ratio predicted by Newtonian theory, outside the vicinity of the stagnation line, was low compared with experimental data. This discrepancy between theoretical and experimental data increased with angle of attack. Newtonian theory, of course, cannot be used to predict the pressure on the expansion (leeward) surfaces. The flow-deflection angle δ gave reasonable predictions for the shift of the stagnation line with angle of attack, and the pressure distribution in the vicinity of the stagnation line was in reasonable agreement with the Newtonian distribution for all test conditions.

It should be pointed out here that when the angle of attack is sufficiently large δ will exceed δ_{max} and the wing panel will influence the location of the stagnation line and the pressure distribution and pressure gradient in the vicinity of the stagnation line. For the present models, δ is greater than δ_{max} at angles of attack of 17.57° and 11.9° for the 0° and 45° dihedral models, respectively. Because of the limited instrumentation on the present models the pressure effect resulting from δ exceeding δ_{max} cannot be discerned.

Since Newtonian theory predicted pressures which were lower than the measured pressures on the wing panel, the tangent-wedge and tangent-cone methods and two variations of a method developed by Creager (refs. 3, 4, and 5), which assumed the pressure on a delta wing could be expressed as a linear combination of viscous and inviscid pressure effects, were employed in an attempt to predict these pressures. For the tangent-wedge method, the flow at an initial Mach number of 4.95 was assumed to be deflected through an angle equal to the wing-panel effective angle of attack. The effective angle of attack is given by the following:

$$\alpha_{eff} = \sin^{-1}(\sin \alpha \cos \Gamma) \tag{5}$$

The tangent-cone method assumed that the pressure on the wing panel inclined to the free-stream velocity by an amount α_{eff} would be equal to that experienced by a cone at zero angle of attack with a semiapex angle equal to α_{eff}.

The first variation of Creager's method, noted as Creager method I, assumed that the asymptotic pressure on the wing panel was equal to the tangent-wedge pressure, whereas the second variation, Creager method II, assumed that the panel pressure ultimately approached the tangent-cone value. The pressures on the expansion surfaces of the wing panels were estimated by using a Prandtl-Meyer expansion and Creager method I with the asymptotic pressure equal to the Prandtl-Meyer value. The Newtonian and Prandtl-Meyer pressures were matched at the sonic point and disregarded the differences in the pressure gradient.

In general, Creager method II gave the best predictions for the pressures on the models for the compression surfaces. However, for the 45° dihedral model at angles of attack of 10°, 15°, and 20°, the asymptotic value of the pressure appeared to be between the tangent-wedge and tangent-cone values. Creager method I gave good estimates for the pressure in the expansion surfaces of the models except for the 45° dihedral model at angles of attack of 15° and 20°, where the theoretical curves were low compared with the experimental data.

Center-Line and Stagnation-Line Pressure Level

The pressure level at the leading-edge center line ($s = 0$) and the stagnation line was evaluated by comparing the measured pressures with the theoretical values obtained from the ideal-gas normal-shock relationship based on the normal component of the free-stream Mach number. The results of these comparisons are presented in figures 5 and 6.

Since the stagnation-line location varied with angle of attack, direct measurement of the stagnation-line pressure was not made. The stagnation-line pressure was calculated from the measured center-line ($s = 0$) pressure data and the theoretical Newtonian pressure distribution by assuming that the stagnation line shifted from $s = 0$ an amount δ. This procedure appeared reasonable since the distributions discussed in the previous section indicated that the shift in the stagnation-line location could be predicted by δ. It might have been desirable to fair through the data to obtain the stagnation-line pressure; however, it was felt that the limited instrumentation available would lead to somewhat arbitrary values for the stagnation-line pressures. The free-stream stagnation pressure was used to nondimensionalize the pressure-level data. The results of these calculations are compared

in figure 6 with the ideal-gas normal-shock pressures obtained from the free-stream normal Mach number.

The leading-edge center-line (s = 0) pressures, presented in figure 5, were nondimensionalized by dividing the measured pressures by the free-stream stagnation pressure. The theoretical curve presented in the figure was obtained from the ideal-gas normal-shock pressure based on the normal component of the free-stream Mach number and accounting for the shift in the stagnation line with angle of attack.

Figures 5 and 6 indicate that the measured center-line and stagnation-line pressure for the 0° and 45° dihedral models agree with the theoretical pressures within ±9 percent. The agreement between the data from stations A and B for the 45° dihedral model is very good. There is, however, a maximum discrepancy of about 11 percent between the data from these two stations for the 0° dihedral model which cannot be explained. L 1 3 2 4

CONCLUDING REMARKS

An experimental investigation was conducted to measure the pressures on two 60° swept delta wings with cylindrical leading edges of 0.25-inch radii and dihedral angles of 0° and 45°. The tests were conducted at a Mach number of 4.95 and a stagnation temperature of 400° F. The test-section unit Reynolds number was 15.19×10^6, and the angle-of-attack range was varied from 0° to 20°.

The results of the investigation indicated that, in general, Newtonian theory could not be used to predict the pressure distribution on the models, in a plane normal to the leading edge, for angles of attack greater than 0° since the theory underestimated the pressure on the wing panel at higher angles of attack. Newtonian theory could, however, be used to estimate the distribution in the vicinity of the stagnation line for the angle-of-attack range investigated. Creager's method, with the use of an asymptotic pressure obtained from the tangent-cone method was, in general, in good agreement with the data obtained from the wing panel with positive inclination to the free-stream velocity. Creager's method, with the use of a Prandtl-Meyer expansion, predicted to good accuracy the measured pressures on the wing panel with negative inclinations.

The stagnation-line pressure level could be predicted within ±9 percent by using the ideal-gas normal-shock relationship with the normal component of the free-stream Mach number.

Langley Research Center,
National Aeronautics and Space Administration,
Langley Air Force Base, February 2, 1962.

REFERENCES

1. Cooper, Morton, and Stainback, P. Calvin: Influence of Large Positive Dihedral on Heat Transfer to Leading Edges of Highly Swept Wings at Very High Mach Numbers. NASA MEMO 3-7-59L, 1959.

2. Stainback, P. Calvin: Heat-Transfer Measurements at a Mach Number of 4.95 on Two 60° Swept Delta Wings With Blunt Leading Edges and Dihedral Angles of 0° and 45°. NASA TN D-549, 1961.

3. Creager, Marcus O.: An Approximate Method for Calculating Surface Pressures on Curved Profile Blunt Plates in Hypersonic Flow. NASA TN D-71, 1959.

4. Creager, Marcus O.: The Effect of Leading-Edge Sweep and Surface Inclination on the Hypersonic Flow Field Over a Blunt Flat Plate. NASA MEMO 12-26-58A, 1959.

5. Creager, Marcus O.: Effects of Leading-Edge Blunting on the Local Heat Transfer and Pressure Distribution Over Flat Plates in Supersonic Flow. NACA TN 4142, 1957.

TABLE I.- GEOMETRY OF MODEL

Model designation	Γ, deg	ϵ_o, deg	Λ_o, deg	ϵ_p, deg	ϵ_n, deg	α_{ϵ_e}, deg	$\Lambda_{e,max}$, deg
0° dihedral model	0	30	60	30	0	90	60
45° dihedral model	45	30	60	20.71	22.21	20.75	69.29

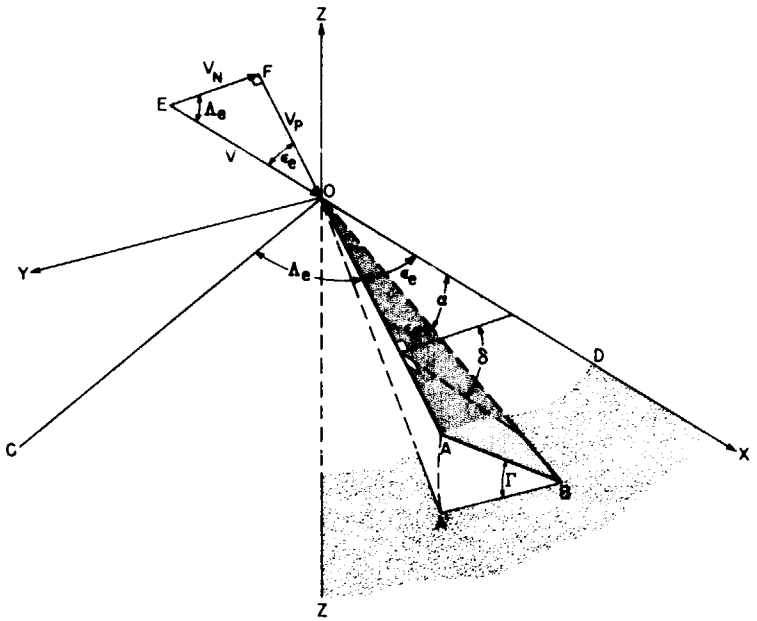

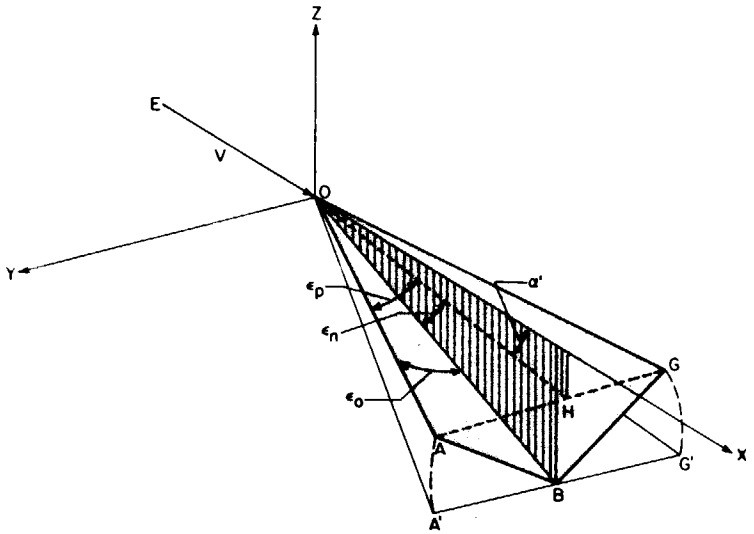

Geometry details

OABG	Wing with dihedral
OA'BG'	Reference plane
OB	Center line of wing located in plane Y = 0
OAB	Plane of wing panel ($Y \geq 0$)
OGB	Plane of wing panel ($Y \leq 0$)
EFODAC	Plane of resultant velocity vector and components V_N and V_P; also plane formed by leading edge of wing (OA) and x axis

Dihedral angle Γ in plane perpendicular to OB

Figure 1.- Wing geometry.

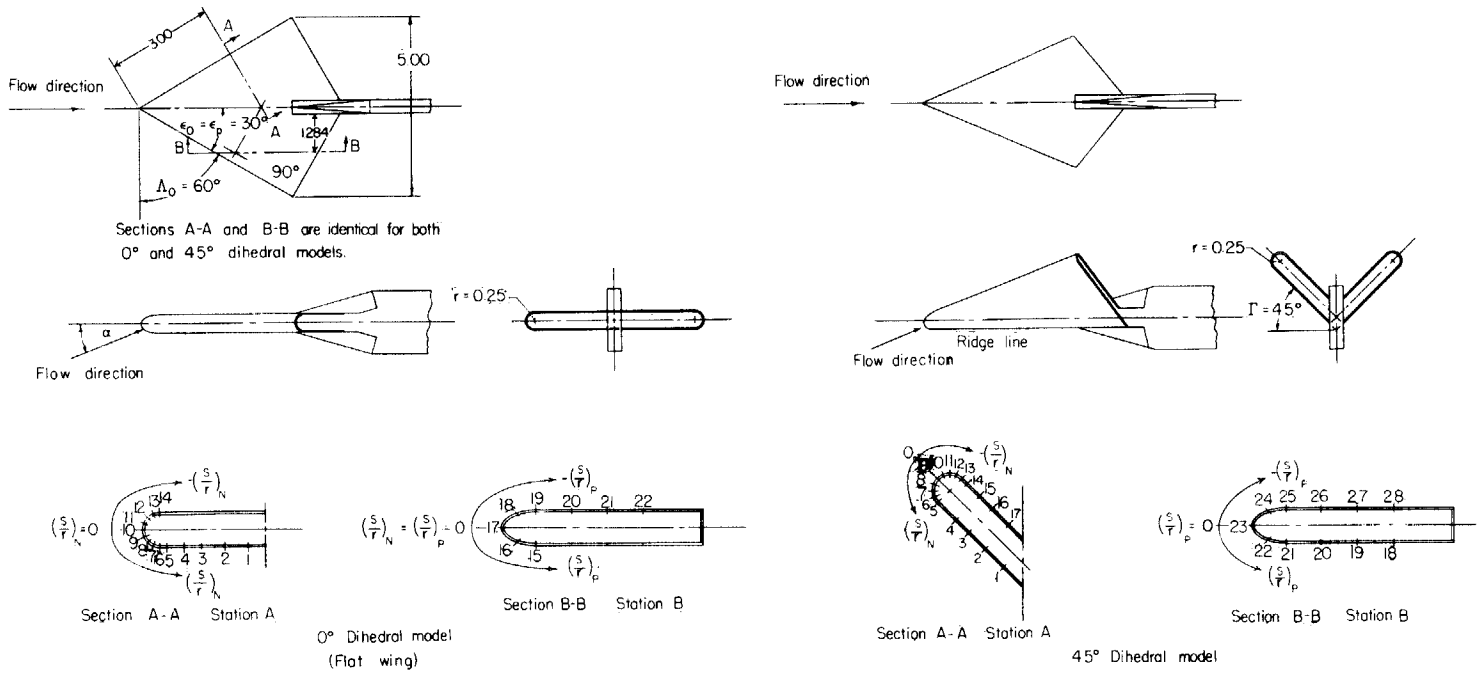

Figure 2.- Geometry and instrumentation of models. The 0° and 45° dihedral models were fabricated from identical wing panels.

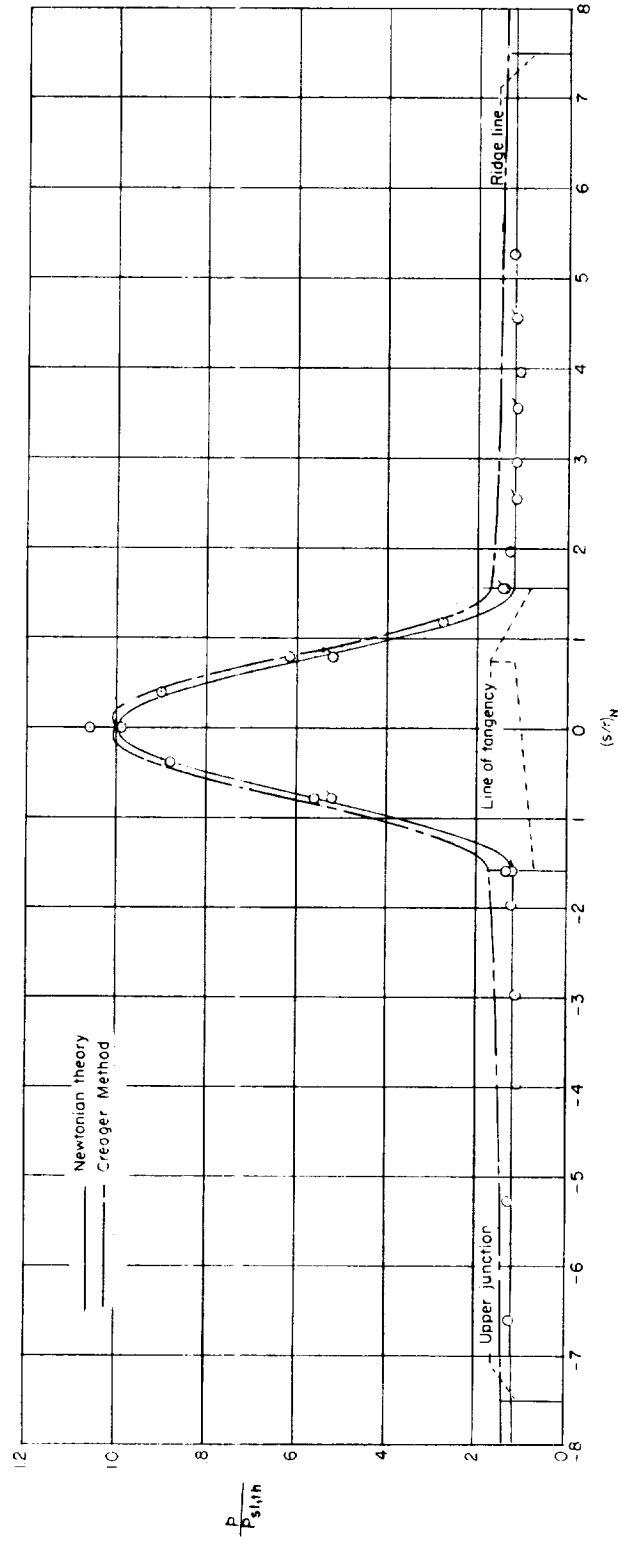

(a) $\alpha = 0^{\circ}$.

Figure 3.- Pressure distribution normal to leading edge for 0° dihedral (flat) wing. Plain symbols denote data from station A; flagged symbols, data from station B.

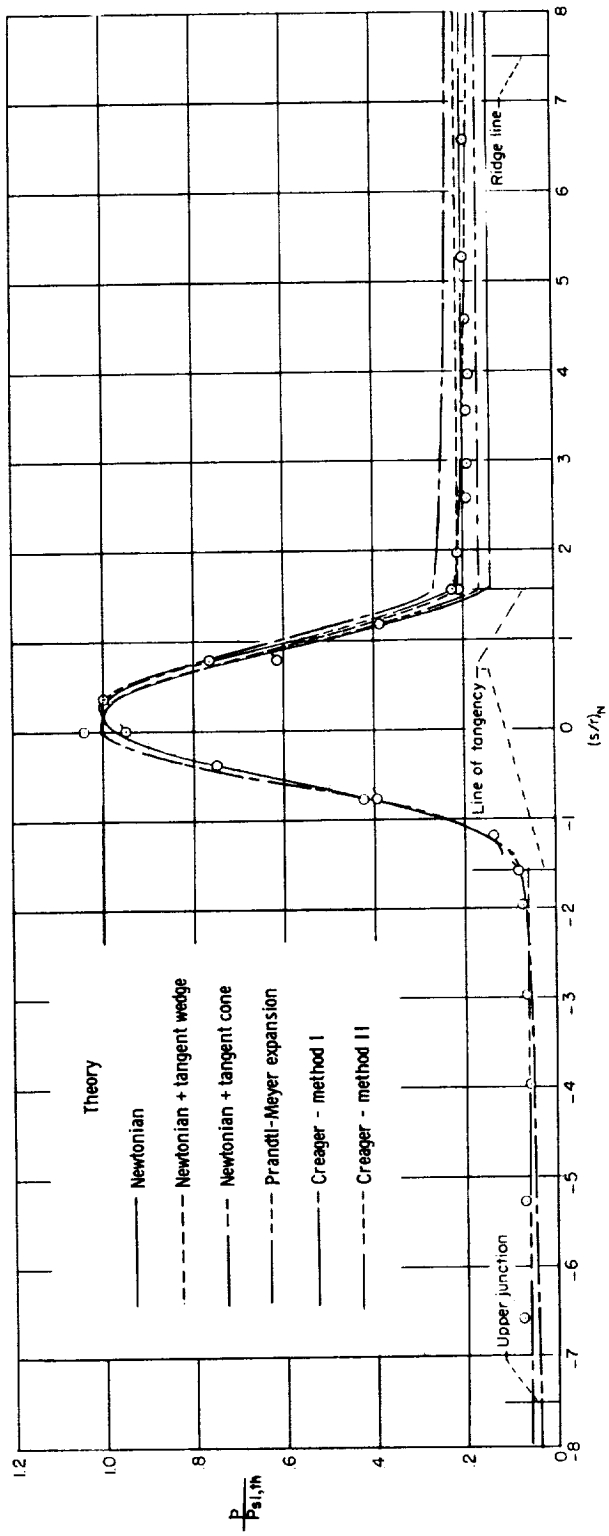

(b) $\alpha = 5^\circ$.

Figure 3.- Continued.

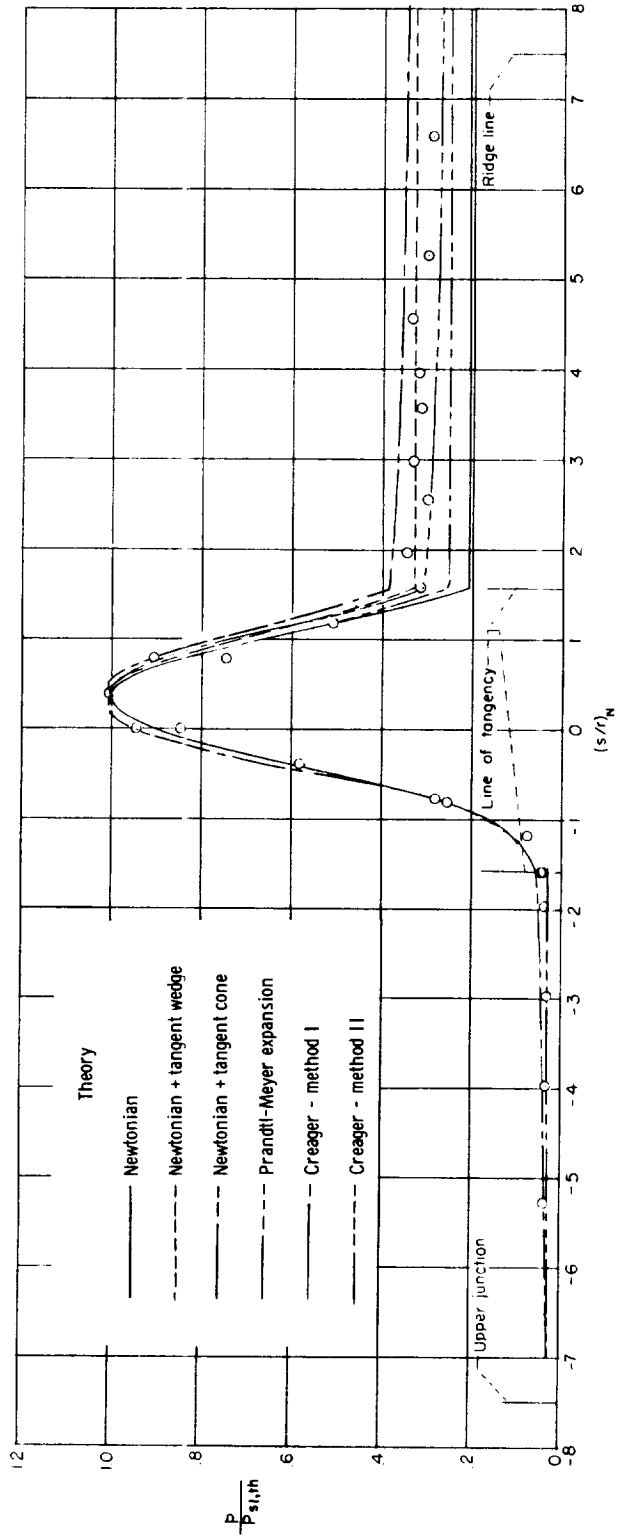

(c) $\alpha = 10^{\circ}$.

Figure 3.- Continued.

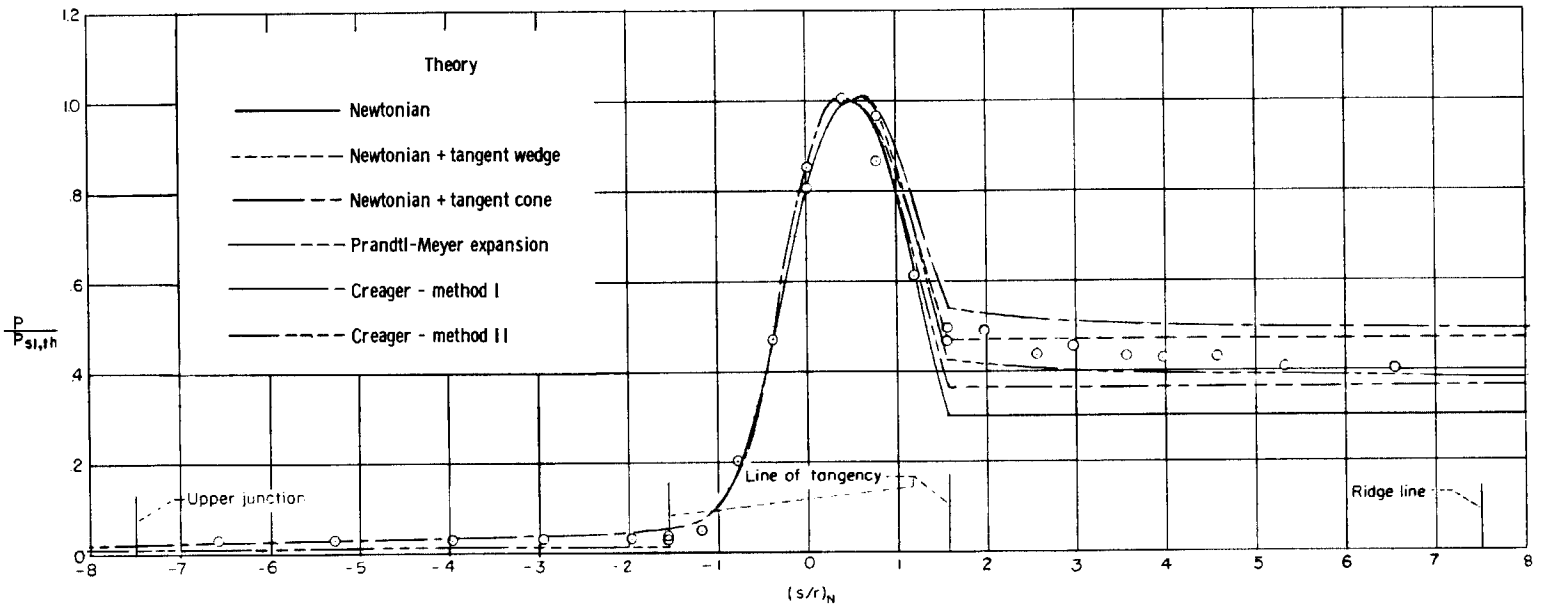

(d) $\alpha = 15^{\circ}$.

Figure 3.- Continued.

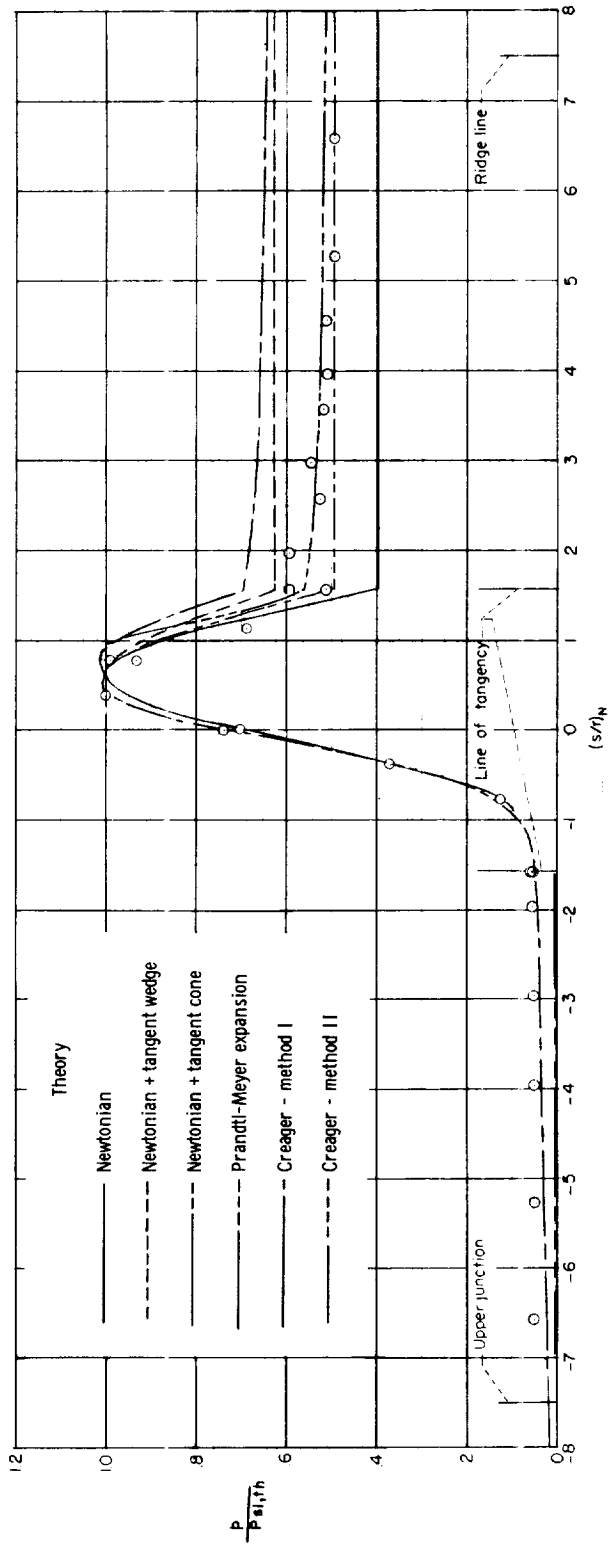

(e) $\alpha = 20^{\circ}$.

Figure 3.- Concluded.

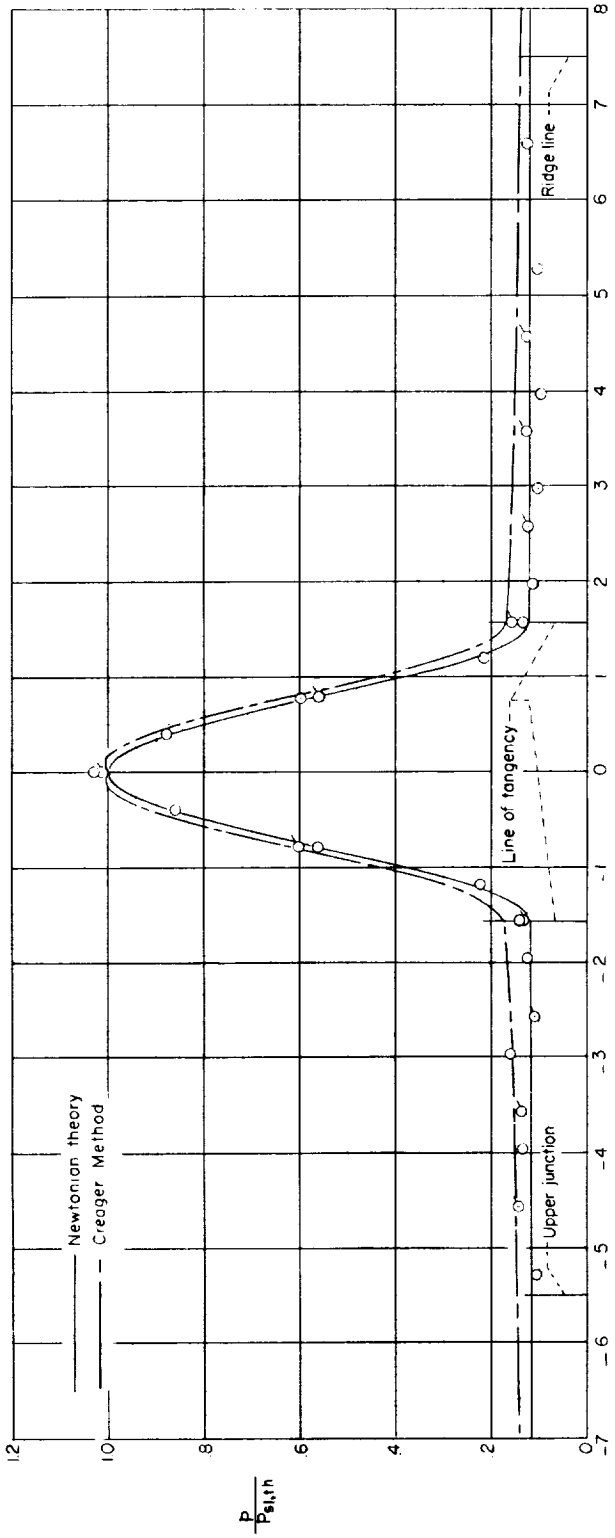

(a) $\alpha = 0^{\circ}$.

Figure 4.- Pressure distribution normal to leading edge for 45° dihedral wing. Plain symbols denote data from station A; flagged symbols, data from station B.

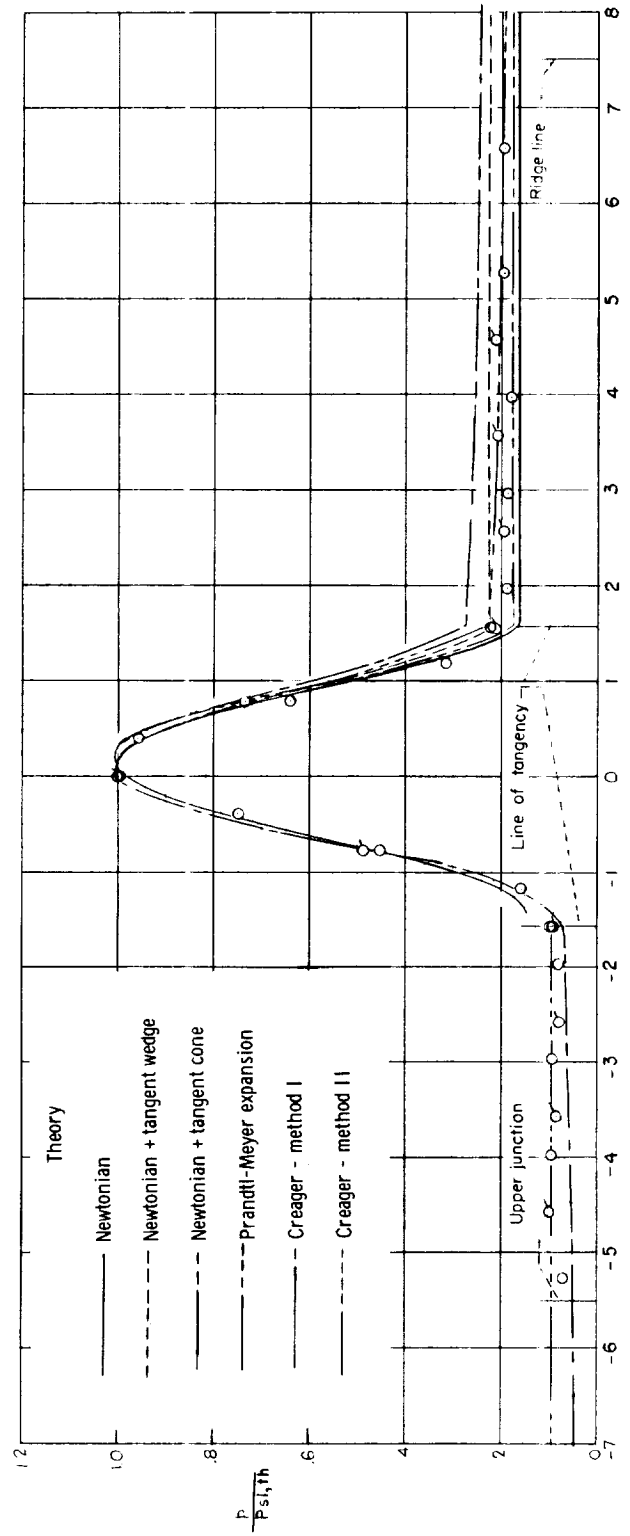

(b) $\alpha = 5^\circ$.

Figure 4.- Continued.

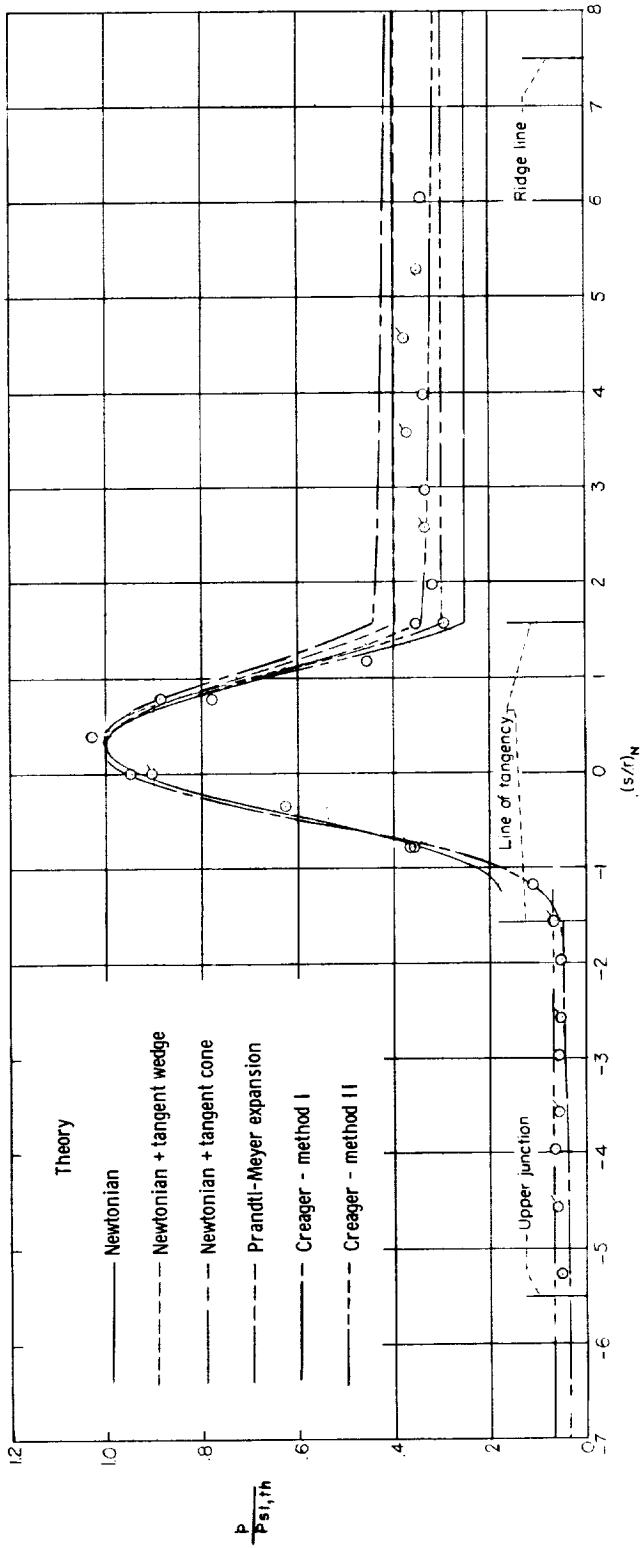

(c) $\alpha = 10°$.

Figure 4.- Continued.

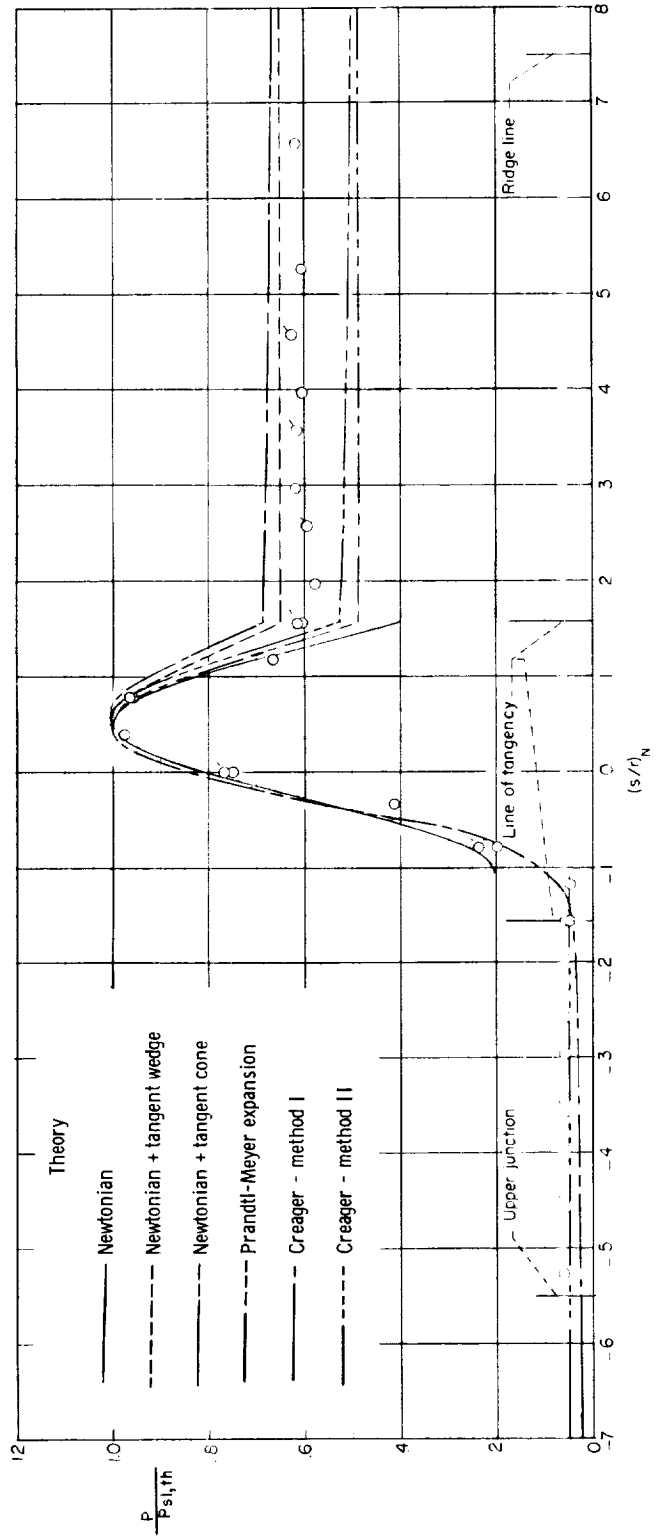

(d) $\alpha = 15^{\circ}$.

Figure 4.- Continued.

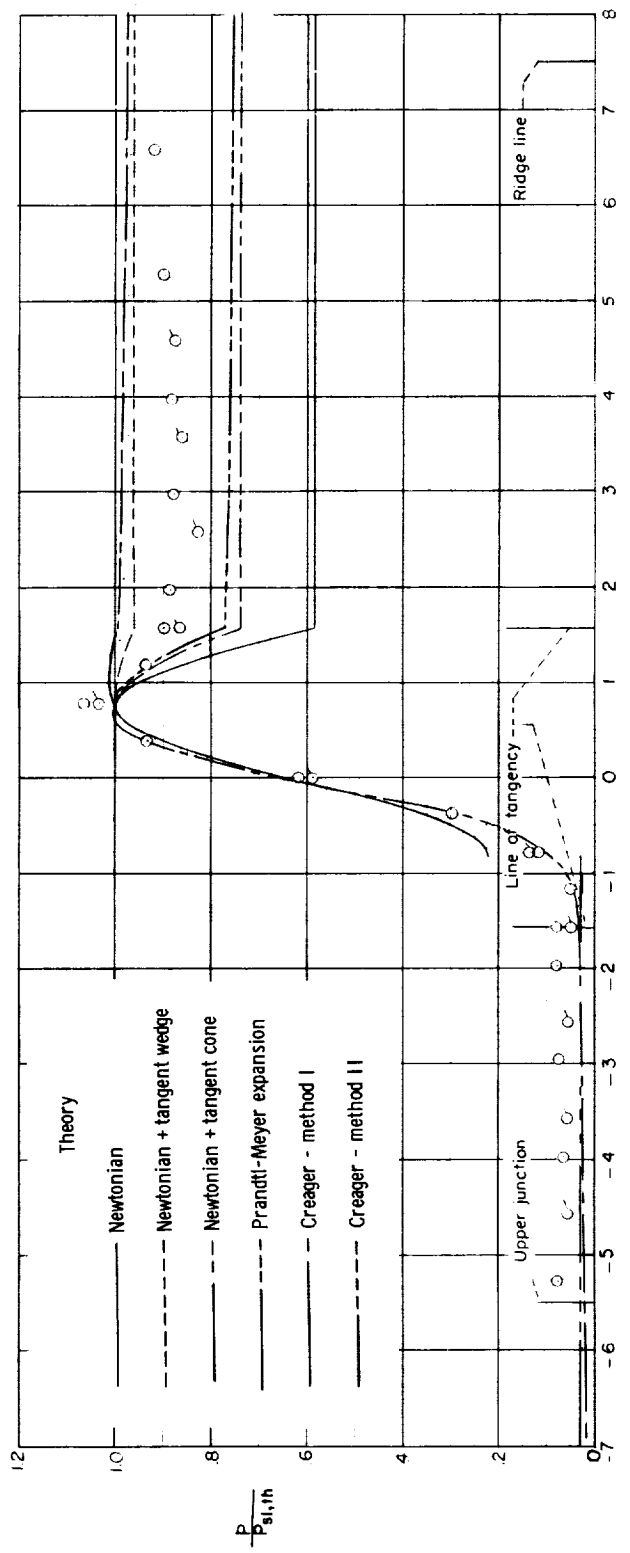

(e) $\alpha = 20^{\circ}$.

Figure 4.- Concluded.

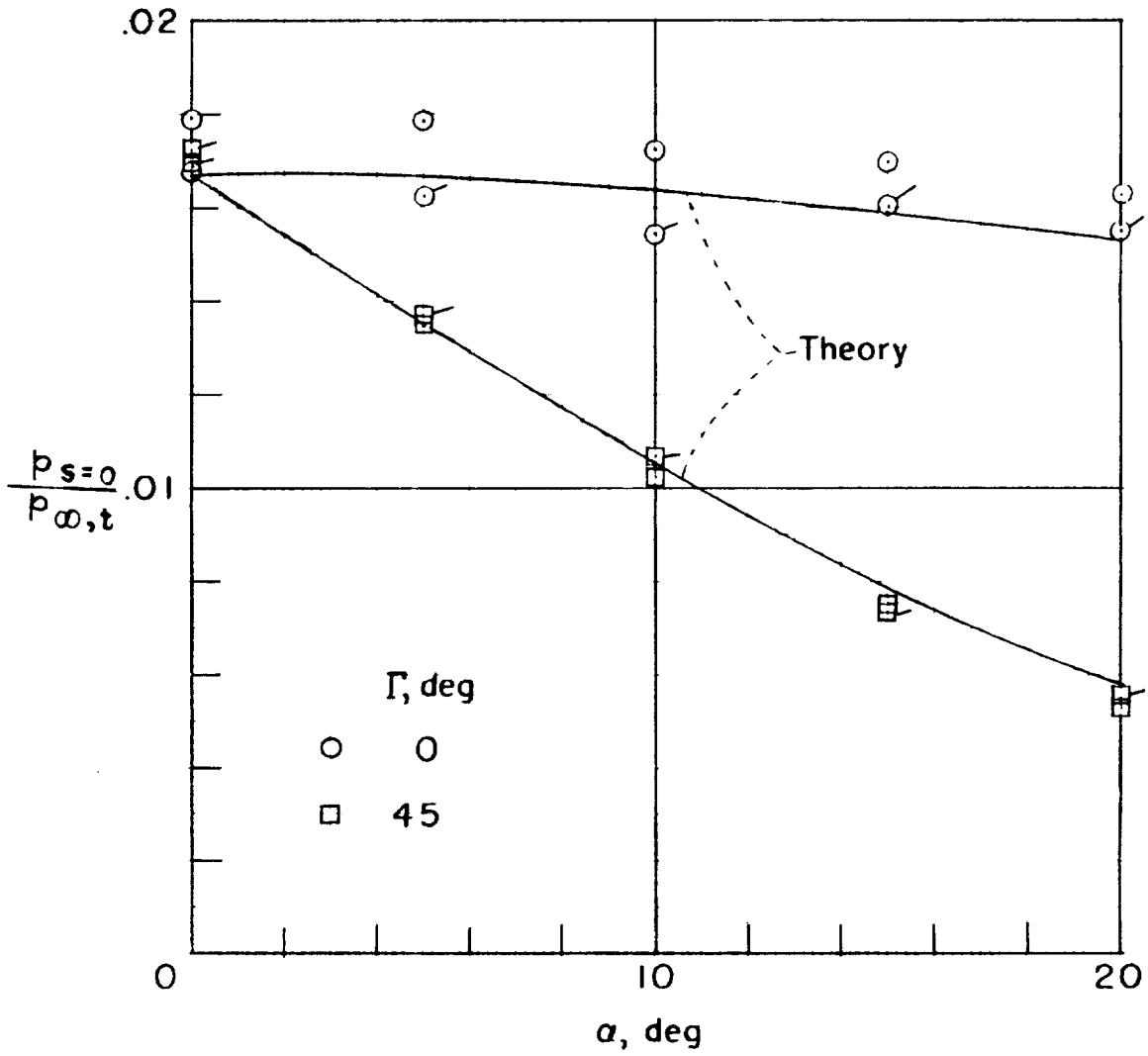

Figure 5.- Pressure level at model leading-edge center line (s = 0). Plain symbols denote data for station A; flagged symbols, data from station B.

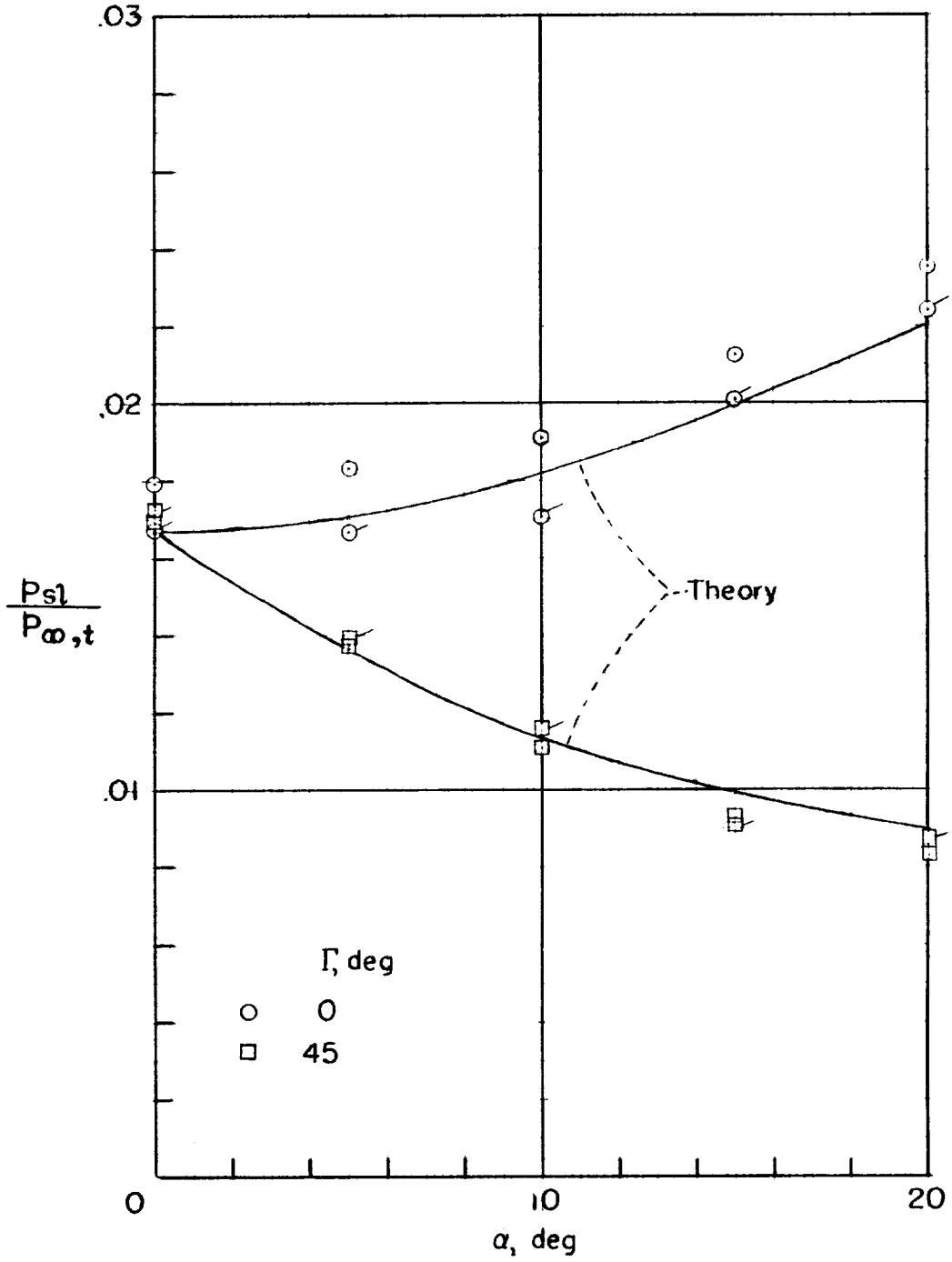

Figure 6.- Pressure level at model leading-edge stagnation line. Plain symbols denote data from station A; flagged symbols, data from station B.

NASA-Langley, 1962 L-1324

L-1324